



## Naturally occurring radioactive material and risk assessment of tailings of polymetallic and Ra/U mines from legacy sites

Isabel Paiva<sup>a, b</sup>, Rosa Marques<sup>a, \*</sup>, Marta Santos<sup>a, b</sup>, Mário Reis<sup>a, b</sup>, Maria Isabel Prudêncio<sup>a</sup>, João Carlos Waerenborgh<sup>a</sup>, Maria Isabel Dias<sup>a</sup>, Dulce Russo<sup>a</sup>, Guilherme Cardoso<sup>a</sup>, Bruno J.C. Vieira<sup>a</sup>, Edgar Carvalho<sup>c</sup>, Carlos Rosa<sup>d</sup>, Daniela Lobarinhas<sup>c</sup>, Catarina Diamantino<sup>c</sup>, Rui Pinto<sup>c</sup>

<sup>a</sup> Centro de Ciências e Tecnologias Nucleares (C2TN), Instituto Superior Técnico, Universidade de Lisboa, EN 10 (km 139.7), 2695-066, Bobadela, Portugal

<sup>b</sup> Laboratório de Protecção e Segurança Radiológica (LPSR), Instituto Superior Técnico, Universidade de Lisboa, EN 10 (km 139.7), 2695-066, Bobadela, Portugal

<sup>c</sup> Empresa de Desenvolvimento Mineiro, SA. (EDM), Rua Sampaio e Pina, n.º 1, 1070-248, Lisboa, Portugal

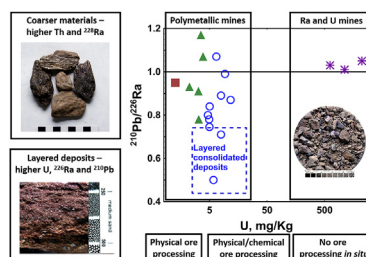
<sup>d</sup> Faculdade de Ciências, Universidade de Lisboa, IDL — Instituto Dom Luiz, Ed. C6, Campo Grande, 1749-016, Lisboa, Portugal



### HIGHLIGHTS

- Th and <sup>228</sup>Ra are more concentrated in the coarser tailings of polymetallic mines.
- Chemical treatments, drainage and deposition may originate high <sup>226</sup>Ra and <sup>210</sup>Pb.
- <sup>222</sup>Rn loss and <sup>226</sup>Ra mobility explain low <sup>210</sup>Pb/<sup>226</sup>Ra values in layered deposits.
- <sup>210</sup>Pb/<sup>226</sup>Ra ≈ 1 and high external outdoor dose rate in surficial Ra, U mine tailings.
- Nano-sized iron oxides may incorporate significant amounts of U and <sup>226</sup>Ra.

### GRAPHICAL ABSTRACT



### ARTICLE INFO

#### Article history:

Received 11 July 2018

Received in revised form

25 January 2019

Accepted 10 February 2019

Available online 11 February 2019

Handling Editor: Martine Leermakers

#### Keywords:

Old mine tailings

NORM

### ABSTRACT

Old mine tailings from Northern and Central Portugal were studied in order to perform a radiological and chemical characterization. The evaluation of massic activity of natural radionuclides and concentrations in tailings of polymetallic and Ra/U mines was performed by gamma spectrometry and neutron activation analysis. Iron speciation was carried out by Mössbauer spectroscopy. In polymetallic tailings with physical ore processing (Cumieira and Verdes - exploited for Sn, Nb-Ta) higher contents of Th, <sup>228</sup>Ra and <sup>226</sup>Ra in the coarser materials occur, probably due to their presence in host rock and ore fragments. In finer tailings, washing may explain the lower <sup>226</sup>Ra and <sup>210</sup>Pb massic activity. In tailings with physical/chemical ore processing (Covas - exploited for W and Sn) high U contents and a tendency for higher <sup>226</sup>Ra and <sup>210</sup>Pb massic activity in the fine materials is observed, probably due to their incorporation in nano-sized particles of iron oxides. A high variation of the <sup>210</sup>Pb/<sup>226</sup>Ra ratio occurs in polymetallic tailings; a deficit of <sup>210</sup>Pb can be observed particularly in deposits of settling tanks drained from dumps of

\* Corresponding author.

E-mail addresses: [ipaiva@ctn.tecnico.ulisboa.pt](mailto:ipaiva@ctn.tecnico.ulisboa.pt) (I. Paiva), [rmarques@ctn.tecnico.ulisboa.pt](mailto:rmarques@ctn.tecnico.ulisboa.pt) (R. Marques), [martasan@ctn.tecnico.ulisboa.pt](mailto:martasan@ctn.tecnico.ulisboa.pt) (M. Santos), [mcapucho@ctn.tecnico.ulisboa.pt](mailto:mcapucho@ctn.tecnico.ulisboa.pt) (M. Reis), [iprudenc@ctn.tecnico.ulisboa.pt](mailto:iprudenc@ctn.tecnico.ulisboa.pt) (M.I. Prudêncio), [jcarlos@ctn.tecnico.ulisboa.pt](mailto:jcarlos@ctn.tecnico.ulisboa.pt) (J.C. Waerenborgh), [isadias@ctn.tecnico.ulisboa.pt](mailto:isadias@ctn.tecnico.ulisboa.pt) (M.I. Dias), [dulcef@ctn.tecnico.ulisboa.pt](mailto:dulcef@ctn.tecnico.ulisboa.pt) (D. Russo), [gcardoso@ctn.tecnico.ulisboa.pt](mailto:gcardoso@ctn.tecnico.ulisboa.pt) (G. Cardoso), [brunovieira@ctn.tecnico.ulisboa.pt](mailto:brunovieira@ctn.tecnico.ulisboa.pt) (B.J.C. Vieira), [edgar.carvalho@edm.pt](mailto:edgar.carvalho@edm.pt) (E. Carvalho), [carlosjprosa@yahoo.com](mailto:carlosjprosa@yahoo.com) (C. Rosa), [daniela.lobarinhas@edm.pt](mailto:daniela.lobarinhas@edm.pt) (D. Lobarinhas), [catarina.diamantino@edm.pt](mailto:catarina.diamantino@edm.pt) (C. Diamantino), [rui Pinto@edm.pt](mailto:rui Pinto@edm.pt) (R. Pinto).

Gamma spectrometry  
INAA  
Mössbauer spectroscopy  
Risk assessment

chemically treated ore. In Ervideira-Mestras tailings (Ra/U exploitation) where no ore process *in situ* was performed, a near equilibrium between  $^{210}\text{Pb}$  and  $^{226}\text{Ra}$  occurs. Dose risk assessment was carried out by calculating external outdoor Annual Effective Dose Rate; the dose rates in air due to terrestrial gamma radiation are low for the polymetallic tailings (<47 nGy/h), and higher for tailings of Ra/U (up to 4130 nGy/h), in the worst scenario.

© 2019 Elsevier Ltd. All rights reserved.

## 1. Introduction

Activities related to the extraction and processing of ores can lead to enhanced levels of naturally occurring radioactive material (NORM) in products, by-products and wastes. Mining activities are responsible for the increase of background gamma radiation levels in and around the mines by exposing NORM to the earth's surface (IAEA, 2002). The radiation levels depend on the local geology, soil properties and geographical features of the area, as well as the commodity mined, the leaching and extraction industrial processes applied. High radiation levels are in general related to igneous rocks, while lower radiation levels are associated to sedimentary rocks (Silver Turyahabwa et al., 2016; UNSCEAR, 2008). The determination of radionuclides distribution and radioactivity levels in the environment surrounding large volume of mine tailings from former mining sites is fundamental to assess the population exposure to radiation, to control the waste residues and to establish strategies for further remediation to mitigate potential health threats (Blasco et al., 2016; Bollhöfer et al., 2014; Carvalho et al., 2007; Kamunda et al., 2016).

The main pathways of human exposure to environmental radioactivity are the result of external exposure due to gamma radiation, internal exposure due to radionuclides inhalation (mainly radon and its decay products), radionuclides ingestion due to food and water intake, and dermal residue contact. The contribution of the different pathways to human's radiation doses depends on the radionuclides release type, radiological, physical and chemical characteristics, soil and climate conditions and exposed population habits (Balonov, 2008; Blanco Rodríguez et al., 2018; Bollhöfer et al., 2014; Carvalho et al., 2014). The current international system of radiation protection distinguishes between three situations: planned, emergency and existing exposures. Optimization of radiation protection in existing exposure situation as in the case of milling and mining tailings, may require the application of countermeasures in order to comply with the general radiological criteria recommended by the International Commission on Radiological Protection (ICRP) for all public exposures (dose limit of 1 mSv/year for all controlled sources) (Balonov, 2008; ICRP, 1991, 1999). According to UNSCEAR (2008), the worldwide mean annual effective radiation dose due to natural radiation is 2.4 mSv with variations between 1 and 10 mSv. Both planned and accidental releases of radionuclides can contribute to the increasing of population and non-humans exposure to higher radiation dose levels, with possible harmful effects in the long-term for the environment as well. Therefore, the evaluation of NORM's mass activity such as  $^{238}\text{U}$ ,  $^{232}\text{Th}$  and  $^{40}\text{K}$  is important for both public and the regulator, since it can provide values for the absorbed doses and, consequently, to estimate the radiological hazards for the populations (Rochedo and Lauria, 2008). This information is also crucial for the industry to implementing better waste treatment and remediation processes and to design adequate monitoring programs.

The *Empresa de Desenvolvimento Mineiro, SA (EDM)* under a concession contract established with the Portuguese State has identified 199 abandoned old mines in Portugal that needed

environmental remediation. One hundred and three have been remediated (Carvalho et al., 2016; EDM website; EDM, 2011). In the frame of the ENVIREE project – “ENVIRONMENTALLY friendly and efficient methods for extraction of Rare Earth Elements from secondary sources”, old mine tailings from Northern and Central Portugal have been evaluated as potential secondary raw materials. Among these tailings are critical waste dumps that incorporate mineral species consisting of radioactive nuclei with lengthy half-lives, which are potential hazard especially when dust is dispersed in the environment. Thus, the assessment of natural radionuclides activities and concentrations in waste dumps with technologically enhanced levels of NORM is necessary. Two important categories of mining waste deposits in Portuguese territory are addressed in this work: metal mining and smelting (particularly Sn and W), and Ra and U mining without processing at the mine site.

The present work is focused on the correlation of the natural radionuclides activities ( $^{40}\text{K}$ , Th and U series) and the total contents in surficial tailing materials in the different types of waste materials, ore, host rocks and processing routes from four milling and mining sites in Northern and Central Portugal – Covas, Cumieira and Verdes mined for W, Sn and Nb-Ta concentrates (COLTAN), and Ervideira-Mestras mined for Ra and U. The dose and risk assessment of the different tailings to the exposed population was also performed, in order to better characterize these mine tailings for potential further remediation.

## 2. Materials and methods

### 2.1. Studied areas, sampling and samples preparation

Surficial materials (0–30 cm depth) from tailings of four abandoned mines located in Northern and Central Portugal (Fig. 1), well documented by EDM records, were sampled during spring 2015. The study sites have a temperate warm climate with the highest rainfall values in winter (mainly in January), July being the driest month. In each tailing area, the selection of the sampling sites was done taking into account: (i) the mining residues and geological characteristics; and (ii) similar topographic and geomorphological conditions, preferentially relatively flat areas, thus avoiding slopes, watercourses and vegetation. The surficial materials collected mainly correspond to tailings, and also a minor proportion of soil mixed during the stockpiles construction. The grain size classification was done according to Wentworth (1922).

The mineralization type, the host and outcropping rocks, the tailing areas and sampling are briefly described as follows:

- Covas (Vilares, Viana do Castelo) (Fig. 1A – mine location 1; Fig. A1 - photographs in supplementary material – Appendix A)
- skarn type, tungsten mineralization (scheelite and minor wolframite), cassiterite, sulphides, apatite, chlorite, muscovite, quartz and iron oxides, exploited for W and Sn; the host and outcropping rocks are pelitic schists, impure marbles, quartzites, aplitic-pegmatitic veins and granite. Floating, roasting and

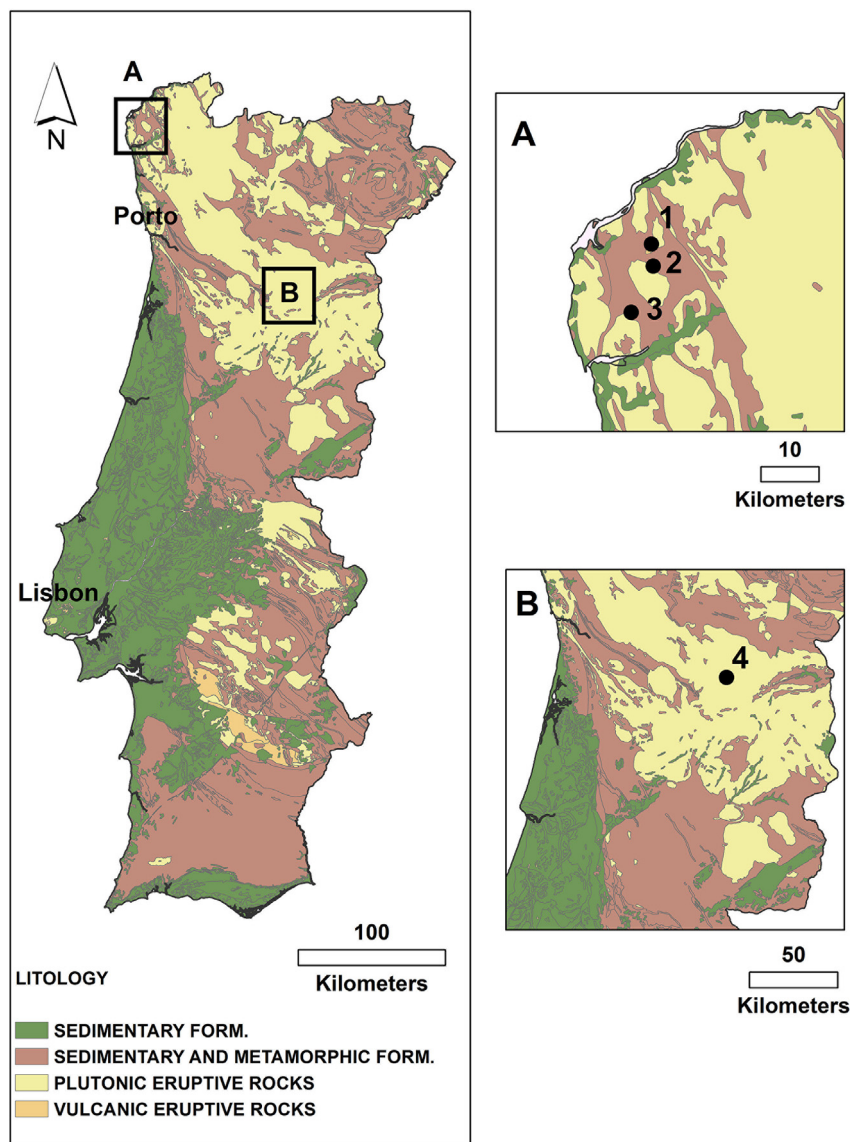


**Fig. 1.** Lithological map with the mine tailings locations. A) polymetallic mines in Northern Portugal: 1- Covas, 2 - Cumieira, and 3 - Verdes, and B) Ra and U mines in Central Portugal: 4 - Ervideira-Mestras.

hydrogravitic mining processes were used. The tailing area was already rehabilitated through slope stabilization, reduction of the pluvial infiltration, limitation of the surface area and use of natural processes for chemical neutralization. Ten samples were collected from three piles of the waste dumps ( $41^{\circ}52'24.40''N$ ;  $8^{\circ}42'19.50''W$ ): (A) - three samples of fine to medium sand (COV A1, A3, A4) and one consisting of coarse sand and fragments (COV A2); (B) five samples collected in the main zone with material from the processing plant: COV B1–B3 - medium sand to fine gravel, COV B4 - consolidated layered sandy material (bottom of a settling tank), COV B5 - coarse sand with aplite fragments; and (C) one sample of very fine (clay to silt) banded material (deposit) from drainage of tailings areas (COV C1).

- Cumieira (Serra de Arga, Caminha) (Fig. 1A - mine location 2; Fig. A2 - photographs in [supplementary material - Appendix A](#)) - placer deposit formed by weathering and accumulation of clasts of schists, quartz, granite and aplite-pegmatite, exploited for Sn and Nb-Ta (COLTAN). Cassiterite grains occur in layers of the elluvial deposit; the host rocks are micaschists with

phosphate nodules. Hydrogravitic and washing processes were used. Two areas with tailings were identified ( $41^{\circ}50'21.86''N$ ;  $8^{\circ}42'4.19''W$ ) and five samples were collected: (i) three samples (CUM A1, CUM B1, CUM C1) of coarse materials from a large area comprising several piles, and (ii) two samples (CUM D1 - D2) of fine materials from the hydrogravitic plant.

- Verdes (Amonde, Viana do Castelo) (Fig. 1A - mine location 3; Fig. A3 - photographs in [supplementary material - Appendix A](#)) - quartz and aplite-pegmatite veins, breccia cemented by quartz and pegmatites with cassiterite, exploited for Sn and COLTAN; the host rocks are metasediments with intercalations of volcanic to volcanoclastic rocks with abundant sulphides. Electromagnetic and hydrogravitic processes were used. The tailing body is integrated in the landscape following the slope/hill side ( $41^{\circ}46'5.38''N$ ;  $8^{\circ}44'46.29''W$ ). One fine grain size sample (VER A1) was collected.
- Ervideira-Mestras (Gradiz, Aguiar da Beira) (Fig. 1B - mine location 4; Fig. A4 - photographs in [supplementary material - Appendix A](#)) - exploited for radium and uranium

(metatorbernite and autunite), the mineralization occurs in polyphasic veins, hosted in basic rocks and in two mica coarse granite. The ore was not processed at the mine site. Most of the tailing of Ervideira sector (nowadays filling the trench and shafts) is integrated in the landscape (40°51'7.62"N; 7°31'31.82"W), consisting of coarse clasts of quartz basic rock and granite. The coarser clasts (up to 5 cm long) are typically coated with metatorbernite (sample ERV 2). The tailing of Mestras sector is integrated in the landscape (40°51'41.86"N; 7°31'57.03"W), consisting of fine to coarse material. The clasts are of granite and quartz. Metatorbernite and rare autunite are abundant coating of the clasts surfaces. Two discrete samples were collected: one of coarse gravel that in general covers the tailing (MEST 1), and one of coarse sand to fine gravel (MEST 2). While Mestras zone is still waiting for intervention within the national program for the rehabilitation of old mining sites, Ervideira zone has already gone through environmental remediation (2008–2009) with the setup of cover materials to reduce background radiation.

Sampling of the tailings materials was done after removal of vegetation and roots. About 10 Kg of each sample was collected with a shovel and hoe, using gloves. The samples were packed into plastic bags and then dried at 30 °C for one week in the laboratory. The samples were homogenized and after a repeated mixing procedure, were quartered by hand. Portions of 2 Kg each were ground in agate mortars and sifted by passing the dry powder through a 63 µm sieve. The powdered samples were homogenized by spinning of a PVC container with milled sample in a mixer during 8 h. Aliquots of each sample were separated and prepared for analyses.

## 2.2. Gamma spectrometry measurements

Natural radionuclides were measured by gamma spectrometry in plastic jar containers of 160 ml volume. The containers were closed and sealed with PVC glue to prevent the leakage of <sup>222</sup>Rn resulting from <sup>226</sup>Ra decay. To accurately quantify the activity of <sup>226</sup>Ra and <sup>228</sup>Ra using their daughter radionuclides, the samples were measured after 30 days, the time lapse needed for the ingrowth of decay products reaching radioactive equilibrium in the sample matrix. The acquisition time was set to 15 h and the photopeaks used for the activity determination were: 1460.82 keV for <sup>40</sup>K, 46.5 keV for <sup>210</sup>Pb, 143.77 keV for <sup>235</sup>U, 295.2, 351.9 and 609.3 keV for <sup>226</sup>Ra and 238.63, 583.19 and 911.20 keV for <sup>228</sup>Ra. A 50% relative efficiency broad energy HPGe detector (Canberra BEGe model BE5030), with an active volume of 150 cm<sup>3</sup> and a carbon window was used for the gamma spectrometry measurements. A lead shield with copper and tin lining shields the detector from the environmental radioactive background. Standard nuclear electronics was used and the software Genie 2000 (version 3.4) was employed for the data acquisition and spectral analysis. The detection efficiency was determined using NIST-traceable multi-gamma radioactive standards (POLATOM Laboratory of Radioactivity Standards) with an energy range from 46.5 to 1836 keV and customized in a water-equivalent epoxy resin matrix (density of 1.15 g cm<sup>-3</sup>) to exactly reproduce the geometries of the samples. GESPECOR software (version 4.2) was used to correct for matrix (self-attenuation) and coincidence summing effects, as well as to calculate the efficiency transfer factors from the calibration geometry to the measurement geometry, whenever needed (Sima et al., 2001). The stability of the system (activity, FWHM, centroid) was checked at least once a week with a <sup>152</sup>Eu certified point source. External QC was assured through the participation in intercomparison exercises organized by international organizations. This technique is accredited according to the ISO/IEC

17025:2005 standard.

## 2.3. Instrumental neutron activation analysis

The chemical analysis was performed by instrumental neutron activation analysis (INAA), in order to obtain the total concentrations of K, Th, U and Fe. The samples were prepared for irradiation by weighing 200–300 mg of powder into cleaned high-density polyethylene vials. Two reference materials were used, namely soil GSS-4 and sediment GSD-9 from the Institute of Geophysical and Geochemical Exploration (IGGE). Reference values were taken from data tabulated by Govindaraju (1994). Irradiation (6 h) of samples and standards was carried out in the core grid of the Portuguese Research Reactor (CTN/IST, Bobadela) at a thermal flux of  $3.96 \times 10^{12} \text{ n cm}^{-2} \text{ s}^{-1}$ ,  $\phi_{\text{th}}/\phi_{\text{epi}} = 96.8$  and  $\phi_{\text{th}}/\phi_{\text{fast}} = 29.8$ . Two aliquots of each standard were used for internal calibration. The spectra were processed using the programs GELI and DAISY, adaptations of GELIAN and DAISY programs (Op de Beeck, 1972, 1974); detectors and all the gamma spectrometer components were calibrated before measurements. Relative precision and accuracy are lower than 5%. More details of this analytical method were published elsewhere (Fernandes et al., 2010; Marques et al., 2011; Prudêncio et al., 2015).

## 2.4. Mössbauer spectroscopy

The <sup>57</sup>Fe Mössbauer measurements on selected samples were recorded at 295 and 4 K in transmission mode using a conventional constant acceleration spectrometer and a 25-mCi <sup>57</sup>Co source in Rh matrix. The velocity scale was calibrated using an  $\alpha$ -Fe foil at room temperature. Isomer shift values, IS, are given relative to this standard. Powdered samples were packed together with lucite powder into perspex holders, in order to obtain homogeneous and isotropic Mössbauer absorbers. The absorber thicknesses were calculated on the basis of the corresponding electronic mass-absorption coefficients for the 14.4 keV radiation, according to Long et al. (1983). The measurements taken at 4 K were obtained with the samples immersed in liquid He in a bath cryostat. The spectra were fitted to Lorentzian lines using a non-linear least-squares method (Waerenborgh et al., 2005).

## 2.5. Dose risk assessment

The main contribution to external exposure results from gamma-emitting radionuclides present in the soil, mainly <sup>40</sup>K and the isotopes from the <sup>238</sup>U and <sup>232</sup>Th natural decay series. The dose risk assessment can be performed on the basis of environmental monitoring data, obtained either from direct measurements of dose rates or from evaluation based on measurements of radionuclides concentration in soils which is the methodology followed in this work. The main quantity used to characterize external exposure fields due to natural sources is the absorbed dose rate in air, usually reported in nanogray per hour (nGy/h). The external doses ( $E_{\text{ext}}$ ) may also be estimated from environmental concentrations of natural radionuclides in soil ( $C_{\text{soil}}$ ) using appropriate dose conversion factors ( $\text{DCF}_{\text{soil}}$ ):

$$E_{\text{ext}} = C_{\text{soil}} \text{DCF}_{\text{soil}} [(1 - I_{\text{in}}) + \text{SF} * I_{\text{in}}] \text{ (nGy/h)} \quad (1)$$

where  $(1 - I_{\text{in}})$  is considered as 0.2, since the world average outdoor and indoor occupancy factors are 0.2 and 0.8 respectively (UNSCEAR, 2000), and the  $\text{DCF}_{\text{soil}}$  are 0.0417, 0.462 and 0.604 for <sup>40</sup>K, <sup>238</sup>U and <sup>232</sup>Th, respectively (UNSCEAR, 2008). In this particular case, since the main objective is to assess outdoor exposures, the fraction of time spent indoors ( $I_{\text{in}}$ ) and the shielding factors of

buildings (SF) were not considered. To estimate the average annual exposure of individuals, external exposures are usually assessed using effective dose rates expressed in units of mSv per year. Thus, the external outdoor Annual Effective Dose Rate ( $E_o$ , mSv/y) for the studied mines was calculated using the equation (UNSCEAR, 2000):

$$E_o = D_o \times DCF \times OF \times T \text{ (mSv/y)} \quad (2)$$

where,  $D_o$ , DCF, OF are the average absorbed dose rate in air (nGy/h), dose conversion factor (0.7 Sv/Gy), outdoor occupancy factor (0.2), respectively, and  $T = 8760$  h, is the annual exposure time. Even considering that some of the sites are close to populated areas and could be accessed by the public, the methodology used is overrated, since it estimates the doses considering populations living over tailings 20% of their daily time (5 h/day), which is not the case.

### 3. Results and discussion

The massic activity of natural radionuclides, as well as the dose rate (total), and the total contents of K, Th and U in surficial samples from tailings of abandoned mines from Northern and Central Portugal are given in Table 1. The values obtained in this work are in agreement with data found in previous studies of abandoned mining areas (Carvalho, 2014; Kamunda et al., 2016; Tuovinen et al., 2016). The degree of oxidation and the fractions of Fe incorporated in the Fe containing phases, shown in Table 2, were deduced from the analysis of the Mössbauer spectra described in detail in the supplementary material (Appendix B).

Chemical contents of uranium clearly distinguish Ervideira-Mestras tailings (Fig. 2A) as expected since uranium tailings, from mining exploitation only, and not from milling process, generally retain 5–10% of the uranium (Vandenhove, 2000). Higher thorium contents were found in coarse samples from Cumieira and Covas tailings (Fig. 2B).

The  $^{40}\text{K}$  massic activity vs. K concentrations are plotted in Fig. 3A, where the significant variations and high contents observed

in tailings are explained by the nature of the ore and host rocks, since potassium is mainly incorporated in feldspars and micas, and in secondary phyllosilicates. In fact, potassium mobility is very low under weathering conditions, and therefore its loss during mineral processing was most probably negligible (Naamoum et al., 2002).

The results obtained for Covas tailings show a significant degree of heterogeneity which may reflect different proportions of the fragments of the original ore and host rocks, as well as mining processes, run-off and deposition, as already described by Valente and Leal Gomes (2009a, 2009b) in other mine of Covas region (Valdarcas mine). In this work it was observed that: (i) pile A - in this tailing zone, Th and  $^{228}\text{Ra}$  concentrations are higher in the coarser samples (Fig. 3B) most likely due to the presence of Th host minerals like thorite, monazite, zircon and/or phosphates in clasts of granite, aplites and mica-schists (particularly in sample COV A2). The same trend was found for K and  $^{40}\text{K}$ , which may indicate the presence of Th minerals in K-feldspars. In fact as reported by Grønlie and Torsvik (1989), thorogummite ( $\text{Th}(\text{SiO}_4)_{1-x}(\text{OH})_4\text{X}$ ) and cheralite ( $(\text{Th}, \text{Ca}, \text{Ce})(\text{PO}_4, \text{SiO}_4)$ ) were found to be major thorium hosting minerals, which occur as dusty, irregular and minute inclusion in K-feldspars in hydrothermal thorium-enriched carbonate veins and breccias in the Møre-Trøndelag Fault Zone (Central Norway). In contrast, uranium content is higher in the finer samples, which may be due to its incorporation in nano-sized iron oxides as referred below for pile B. A tendency for  $^{226}\text{Ra}$  and  $^{210}\text{Pb}$  to be less concentrated in the coarser samples is also observed. Nevertheless  $^{235}\text{U}$  massic activity does not appear to be correlated with the grain size; (ii) pile B - in this largest tailing zone, a tendency for low contents of Th and  $^{228}\text{Ra}$  in all samples was found. Potassium contents and  $^{40}\text{K}$  massic activity vary significantly. All the other radionuclides decrease with the increase of the grain size. The U contents and the massic activity of the radionuclides of the U series are higher in the finer samples as observed in pile A. This can be partially explained by their sorption on nano-sized particles of goethite and hematite (Table 2) as well as by their incorporation into distorted, octahedrally coordinated sites, replacing Fe(III) in these nano-sized oxides, as reported by Marshall et al. (2017) and

**Table 1**

Massic activity of natural radionuclides obtained by gamma spectrometry, as well as the dose rates (total), and the total contents of K, Th and U obtained by INAA in surficial samples from the mine tailings of Northern and Central Portugal.

| Sample reference            | Gamma spectrometry Massic activity (Bq Kg <sup>-1</sup> ± U; k = 2 <sup>a</sup> ) |                   |                   |                   |                  | Dose rate Total (nGy/h) <sup>b</sup> | INAA <sup>c</sup> Mass fraction (mg Kg <sup>-1</sup> ) |        |       |      |
|-----------------------------|---|-------------------|-------------------|-------------------|------------------|--------------------------------------|--|--------|-------|------|
|                             | <sup>40</sup> K   | <sup>210</sup> Pb | <sup>226</sup> Ra | <sup>228</sup> Ra | <sup>235</sup> U |                                      | K  | Th     | U     |      |
| Covas                       | COV A1  | 917 ± 65          | 126 ± 21          | 158 ± 11          | 32.2 ± 4.0       | 7.70 ± 3.9                           | 38   | 26,565 | 6.86  | 4.68 |
|                             | COV A2  | 783 ± 54          | 59.0 ± 11         | 75.9 ± 5.6        | 58.3 ± 5.2       | 3.90 ± 1.9                           | 26   | 23,244 | 14.3  | 4.92 |
|                             | COV A3  | 314 ± 25          | 17.9 ± 6.8        | 20.2 ± 2.2        | 12.2 ± 2.0       | n.d.                                 | 7.6  | 8717   | 2.50  | 7.9  |
|                             | COV A4  | 713 ± 50          | 80.0 ± 14         | 95.2 ± 6.9        | 16.9 ± 2.3       | 7.60 ± 3.0                           | 24   | 18,678 | 3.36  | 5.02 |
|                             | COV B1  | 953 ± 67          | 99.0 ± 19         | 114 ± 8.4         | 3.70 ± 1.6       | 8.70 ± 2.9                           | 28   | 32,127 | 0.992 | 11.6 |
|                             | COV B2  | 810 ± 59          | 104 ± 18          | 96.8 ± 7.3        | 8.60 ± 2.2       | 7.30 ± 2.7                           | 26   | 22,248 | 1.60  | 6.56 |
|                             | COV B3  | 546 ± 38          | 56.6 ± 9.7        | 75.9 ± 5.5        | 16.1 ± 1.6       | 4.80 ± 2.4                           | 19   | 15,358 | 3.09  | 4.97 |
|                             | COV B4  | 184 ± 15          | 15.9 ± 4.9        | 31.8 ± 2.5        | 11.3 ± 1.6       | n.d.                                 | 7.3  | 7754   | 2.61  | 5.85 |
|                             | COV B5  | 825 ± 57          | 210 ± 30          | 213 ± 15          | 5.60 ± 1.5       | 17.1 ± 2.5                           | 47   | 25,402 | 1.26  | 9.27 |
|                             | COV C1  | 256 ± 20          | 67.0 ± 11         | 94.5 ± 6.8        | 34.3 ± 3.5       | 5.30 ± 2.0                           | 21   | 7272   | 8.34  | 7.90 |
| Cumieira                    | CUM A1  | 538 ± 40          | 70.0 ± 13         | 59.9 ± 4.8        | 55.0 ± 5.3       | n.d.                                 | 23   | 16,935 | 14.1  | 3.54 |
|                             | CUM B1  | 1047 ± 73         | 74.0 ± 13         | 69.4 ± 5.5        | 56.3 ± 5.4       | n.d.                                 | 29   | 33,206 | 14.7  | 3.86 |
|                             | CUM C1  | 722 ± 51          | 44.0 ± 11         | 56.4 ± 4.7        | 64.0 ± 5.9       | n.d.                                 | 23   | 21,501 | 14.9  | 3.24 |
|                             | CUM D1  | 632 ± 78          | 36.0 ± 10         | 38.9 ± 5.2        | 17.3 ± 3.1       | n.d.                                 | 14   | 19,757 | 5.48  | 2.23 |
|                             | CUM D2  | 613 ± 44          | 43.0 ± 11         | 47.3 ± 3.8        | 11.0 ± 2.1       | n.d.                                 | 15   | 16,852 | 2.6   | 3.20 |
| Verdes<br>Ervideira-Mestras | VER A1  | 585 ± 43          | 66.0 ± 13         | 69.5 ± 5.3        | 7.50 ± 1.9       | 6.70 ± 3.2                           | 18   | 15,109 | 1.78  | 1.27 |
|                             | ERV 2   | 368 ± 69          | 9161 ± 1193       | 8916 ± 605        | 20.5 ± 5.3       | 603 ± 50                             | 1676   | 11,041 | 4.67  | 6.22 |
|                             | MEST 1  | 237 ± 109         | 22,876 ± 3752     | 21,776 ± 2634     | 21.1 ± 4.6       | 1478 ± 184                           | 4130   | 12,452 | 3.97  | 2220 |
| MEST 2                      | 364 ± 98  | 9223 ± 1514       | 9140 ± 1105       | 16.2 ± 3.1        | 715 ± 90         | 1702                                 | 11,207   | 3.92   | 1111  |      |

n.d. Not detected.

<sup>a</sup> U is the combined uncertainty with an expansion factor of 2.

<sup>b</sup> Dose rate values calculated through Eq. (1).

<sup>c</sup> Coefficient variations better than 5%.

**Table 2**  
Fraction of Fe atoms in the 2 + and 3 + oxidation states, incorporated in the Fe-containing phases, estimated from the Mössbauer spectra taken at 4 K of mine tailing samples from Covas, Cumieira and Mestras (Northern and Central Portugal).

| Sample | % Fe | %Fe <sup>3+</sup> | %Fe <sup>3+</sup> silicate | %Fe <sup>2+</sup> silicate | %Fe <sup>2+</sup> hydrate sulphate | %Fe <sup>2+</sup> arsenopyrite | %Fe <sup>2+</sup> calchopyrite | %nso goethite | %nso hematite |
|--------|------|-------------------|----------------------------|----------------------------|------------------------------------|--------------------------------|--------------------------------|---------------|---------------|
| COV B3 | 7.55 | 79                | 20                         | 14                         | 7                                  | –                              | –                              | 59            | –             |
| COV B4 | 25.2 | 85                | 33                         | 4                          | 5                                  | 6                              | –                              | 33            | 19            |
| CUM D1 | 1.78 | 75                | 19                         | 25                         | –                                  | –                              | –                              | 56            | –             |
| CUM D2 | 1.04 | 80                | 24                         | 20                         | –                                  | –                              | –                              | 56            | –             |
| MEST 2 | 1.66 | 22                | 10                         | 53                         | –                                  | 15                             | 10                             | –             | 12            |

Fe<sub>2</sub>O<sub>3</sub> T total Fe concentration; %Fe<sup>3+</sup> fraction of the total Fe in the 3 + oxidation state; %Fe<sup>3+</sup> silicates, fraction of the Fe in silicates in the 3 + oxidation state; %nso, fraction of the total Fe in nano-sized Fe oxides.

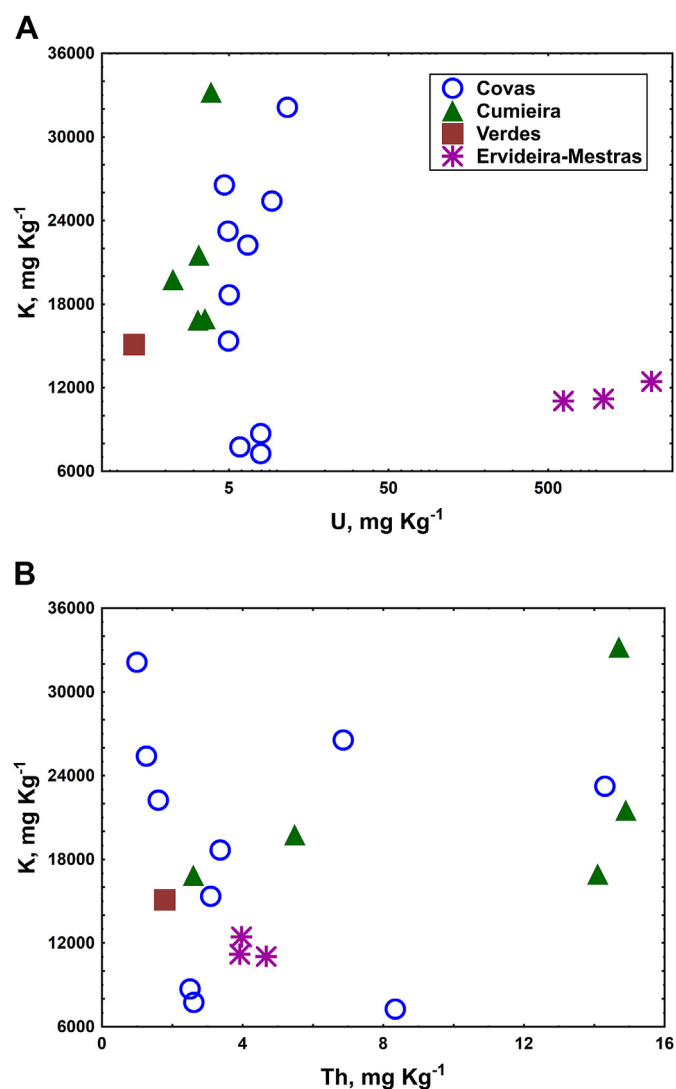


**Fig. 2.** Biplots of (A) K vs. U contents, and (B) K vs. Th contents in polymetallic, Ra and U mine tailings of Northern and Central Portugal (Error bars are smaller than the size of the symbols. See uncertainties in Table 1).

Valente et al. (2015); and (iii) pile C – the radionuclides studied (except <sup>40</sup>K), Th and U appear to be concentrated in this fine deposit, which may be explained by drainage from other tailing areas.

The Cumieira tailings have higher Th contents and <sup>228</sup>Ra massic activity (Fig. 3B) in the coarser samples (CUM A1 – CUM C1). Despite a similar U content in the coarser and finer samples, a similar tendency for higher <sup>226</sup>Ra in the coarser samples was found (Table 1). Since no record of any chemical process of the ore exists,

the high contents found can be due to the presence of these chemical elements and radionuclides in the host rock and ore fragments, probably as complex Th, <sup>226</sup>Ra and U oxides and/or phosphate minerals. During weathering as well as the gravitational movement or accumulation that originate the eluvial deposit, Th may have been less released from the coarser clasts, probably due to its conservative behavior when compared to U, which is in similar amounts in all samples. Furthermore, the hydrogravitic and washing processes used to concentrate the ore may explain the relative lower massic activity of <sup>226</sup>Ra and <sup>210</sup>Pb in the finer samples. 75% to 80% of the total iron is present as Fe<sup>3+</sup>, and 56% occur as nano-sized goethite (Tables 2 and B1), which may accommodate part of U in Cumieira tailings.

The Verdes fine tailing (sample VER A1), resulting from electromagnetic and hydrogravitic processes, is characterized by general low contents of Th and <sup>228</sup>Ra massic activity (Fig. 3B); U content is the lowest found in all tailing samples studied in this work probably due to the uranyl ion mobility (Fig. 3C); nevertheless the <sup>210</sup>Pb and <sup>226</sup>Ra massic activity are within the values found for polymetallic tailings.

Potassium and Th contents, and <sup>40</sup>K and <sup>228</sup>Ra massic activities in the tailing samples of the Ervideira-Mestras mining site are similar. Very high values of U, <sup>226</sup>Ra and <sup>210</sup>Pb were found (Fig. 3C and Table 1). According to Vandenhove (2000), uranium mill tailings generally retain up to 85% of the total activity. For instance, high massic activity of <sup>226</sup>Ra (4000–60,000 Bq Kg<sup>-1</sup>) were reported by Abdelouas (2006) for French uranium mill tailings. The results obtained in this work revealed significant differences in both sectors. The Ervideira sample has lower U content when compared to Mestras, but <sup>226</sup>Ra and <sup>210</sup>Pb values are similar to the finer sample of Mestras (MEST 2) (Table 1). These differences may indicate a former more efficient extraction of U from metatorbernite mineralization in weathered basic rocks than from metatorbernite and autunite hosted in polyphasic veins with quartz. Furthermore, uranyl ions coprecipitation with autunite may play a role in the U stabilization in tailings disposal sites (Abdelouas et al., 1998, 2000; Ohnuki et al., 2004). The Mestras coarser sample (MEST 1) has the highest U content, 2220 mg kg<sup>-1</sup>, and also the highest <sup>226</sup>Ra and <sup>210</sup>Pb massic activity, 21,776 ± 2634 Bq Kg<sup>-1</sup> and 22,876 ± 3752 Bq Kg<sup>-1</sup>, respectively, which may be explained by their presence in phases retained (confined or trapped within closed pore spaces) inside the larger clasts. Incorporation in nano-sized hematite (12% of the total iron in sample MEST 2) can also contribute to the high concentrations found.

The massic activity of <sup>228</sup>Ra, member of the Th series, are lower than those found for <sup>226</sup>Ra in Ervideira-Mestras (Fig. 3B and C), indicating that the ores exploited in these mines are poor in thorium minerals, as already reported by Carvalho et al. (2007) for other radium and uranium mining sites of Portugal. Concerning <sup>228</sup>Ra and <sup>40</sup>K, the massic activity found in tailings of old Ra and U mines are within the range of values observed for the tailings of polymetallic old mines here studied (Table 1).

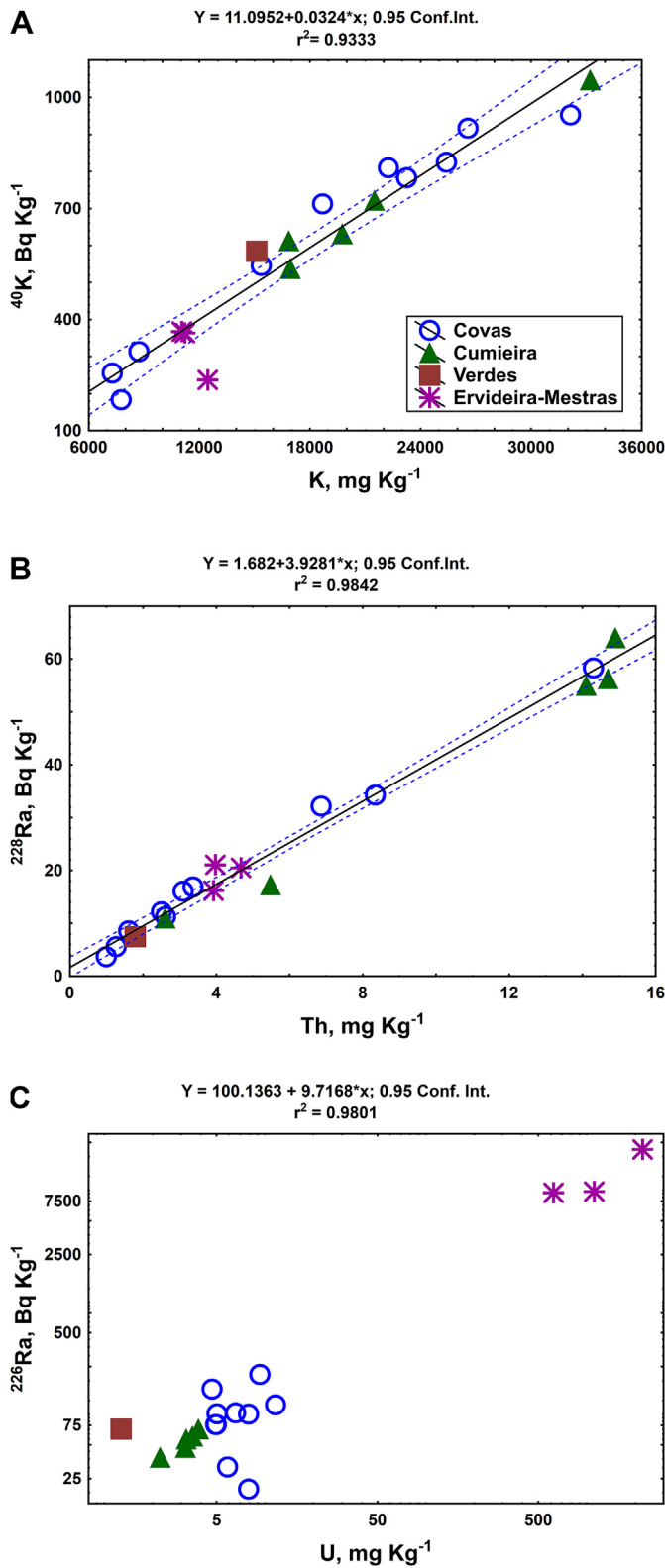


Fig. 3. Biplots of (A)  $^{40}\text{K}$  massic activity vs. K content, (B)  $^{228}\text{Ra}$  massic activity vs. Th content, and (C)  $^{226}\text{Ra}$  massic activity vs. U content in polymetallic, Ra and U mine tailings of Northern and Central Portugal (Error bars are smaller than the size of the symbols. See uncertainties in Table 1).

The  $^{210}\text{Pb}/^{226}\text{Ra}$  ratios vs. U concentrations of all the tailing samples studied in this work are plotted in Fig. 4. The near equilibrium between  $^{210}\text{Pb}$  and  $^{226}\text{Ra}$  in Ervideira-Mestras tailings ( $^{210}\text{Pb}/^{226}\text{Ra} = 1.01\text{--}1.05$ ) confirms the secular equilibrium state between most nuclides of the  $^{238}\text{U}$  decay chain, as well as their stability under the environmental conditions of the tailings. In tailings of polymetallic mines, which consist of a mixture of ore debris, fragments of host rocks and remains of several processing routes, a high variation of the  $^{210}\text{Pb}/^{226}\text{Ra}$  ratio was found, particularly in Covas. The  $^{210}\text{Pb}/^{226}\text{Ra}$  ratio slightly higher than 1 observed for CUM A1, CUM B1 and COV B2 samples may be due to  $^{210}\text{Pb}$  atmospheric deposition (unsupported). This means that its surplus may be attributed to  $^{222}\text{Rn}$  gas diffusion from surrounding waste dumps after entering the atmosphere. When it decays to  $^{210}\text{Pb}$  this isotope is quickly attached to aerosol particles, further precipitating by wet or dry deposition and providing an input of  $^{210}\text{Pb}$  to surface soils. The deficit of  $^{210}\text{Pb}$  with respect to the expected supported  $^{210}\text{Pb}/^{226}\text{Ra}$  ratio observed, particularly in samples COV B4 and COV C1 (consisting of layered deposits resulting from transport/drainage of the tailing area) may be mainly attributed to significant losses of  $^{222}\text{Rn}$  during transport and also due to  $^{226}\text{Ra}$  mobility. In this case,  $^{210}\text{Pb}$  atmospheric deposition did not compensate for the losses (Rodríguez et al., 2014).

The theoretically calculated outdoor absorbed dose rates in air due to terrestrial gamma radiation were found to be low for all the studied tailings resulting from polymetallic mining (from 7 nGy/h up to 47 nGy/h, corresponding to an average effective dose of 0.14 mSv/y). These dose rates are comparable to the average external terrestrial radiation doses reported for sites of different countries (Akhtar et al., 2005; Karahan and Bayulken, 2000; Khatun et al., 2013; Mora et al., 2007) and to the worldwide average outdoor dose rate of 58 nGy/h (UNSCEAR, 2008). In the case of the tailings of Ra and U abandoned mines (Ervideira-Mestras), the estimated values of outdoor dose rates in air are much higher - 1676 nGy/h to 4130 nGy/h, corresponding to an average effective dose of 15 mSv/y, which is in agreement with data expected from uranium tailings areas and other type of mine tailings (Kamunda et al., 2016; Usikalu et al., 2011). These results are consistent with the high annual ambient dose equivalent, reaching  $32 \pm 11$  mSv/y, found by Carvalho et al. (2007) at the milling station of mining facilities of Urgeiriça, uranium mining site in Central Portugal. However, it should be stressed that these doses were calculated by using

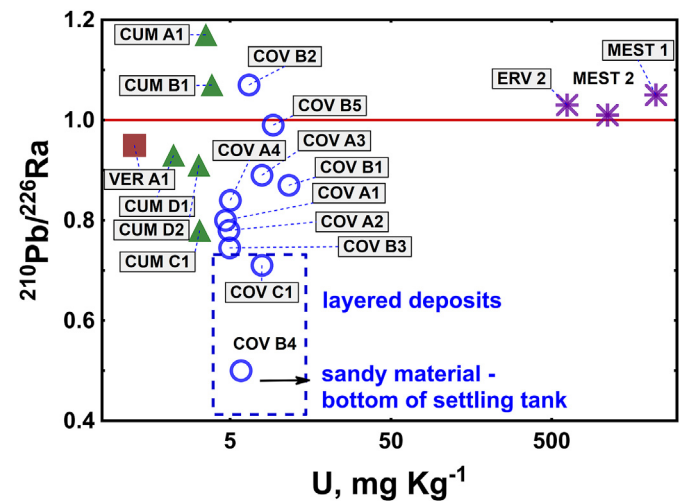


Fig. 4. Biplot of  $^{210}\text{Pb}/^{226}\text{Ra}$  ratio vs. U content in polymetallic, Ra and U mine tailings of Northern and Central Portugal (Error bars are smaller than the size of the symbols. See uncertainties in Table 1).

samples collected in the tailings areas with higher radioactivity, so corresponding to the worst scenario, and should not be directly compared to the effective dose limit for members of the general population, 1 mSv/y, since these areas are not easily accessible to the public.

#### 4. Conclusions

The massic activity of natural radionuclides and the contents of K, Th and U in tailings of abandoned old mines (polymetallic and radioactive ores) show significant variations. In the polymetallic mine wastes (Northern Portugal) left over after physical ore processing, a tendency for higher contents in the coarser tailings of Th,  $^{228}\text{Ra}$ , and at a lower extent  $^{226}\text{Ra}$ , is observed, which may be related to their presence in the waste rock, probably as complex oxides and/or phosphate minerals. Uranium contents are low and do not appear to vary significantly with the grain size probably due to the uranyl ion mobility. A similar behavior was observed for the fine tailings, where low  $^{226}\text{Ra}$  and  $^{210}\text{Pb}$  massic activity are observed, which may be due to washing processes and the low nano-sized iron oxides proportion of these tailings. Tailings resulting from physically and chemically processed ore to concentrate metals also show a tendency for higher Th and  $^{228}\text{Ra}$  in the coarser materials. On the other hand U shows a different behavior: higher U contents occur in the fine tailings probably retained in nano-sized iron oxides, particularly in the layered deposit of settling tanks. A tendency for higher  $^{226}\text{Ra}$  and  $^{210}\text{Pb}$  massic activity in the fine tailings is also observed; nevertheless a high variation of the  $^{210}\text{Pb}/^{226}\text{Ra}$  ratio occurs. A deficit of  $^{210}\text{Pb}$  with respect to the expected supported  $^{210}\text{Pb}/^{226}\text{Ra}$  ratio may be mainly attributed to significant losses of  $^{222}\text{Rn}$  during transport and also due to  $^{226}\text{Ra}$  mobility. In Ra and U mine tailings (Central Portugal), where no ore processing was performed *in situ*, the near equilibrium between  $^{210}\text{Pb}$  and  $^{226}\text{Ra}$  confirms the secular equilibrium state between most nuclides of the  $^{238}\text{U}$  decay chain, as well as their stability under the environmental conditions of the tailings. The outdoor absorbed dose rates in air due to terrestrial gamma radiation were found to be low for all the polymetallic tailings. In the case of Ra and U tailings the dose rates theoretically estimated are much higher, but correspond to the worst scenario of areas not accessible to the public. Nevertheless this assessment is crucial to establish further treatment and remediation strategies in order to avoid dispersion of radioactivity, and mitigate radiological exposure of population in surrounding areas of mine tailings.

#### Acknowledgments

The research was funded by Fundação para a Ciência e a Tecnologia through the project ENVIREE – “ENVIRONMENTALLY FRIENDLY AND EFFICIENT METHODS FOR EXTRACTION OF RARE EARTH ELEMENTS FROM SECONDARY SOURCES”, ERA-MIN/0005/2014 (2015–2017) and UID/Multi/04349/2013 project. The authors would also thank to EDM for their support. The authors gratefully acknowledge Eva Andrade for the conception of the georeferenced samples map. Grateful acknowledgments are made to the Laboratory of Nuclear Engineering (LEN) and also to the staff of the Portuguese Research Reactor (RPI) of CTN/IST for their assistance with the neutron irradiations.

#### Appendices A and B. Supplementary data

Supplementary data related to this article can be found at <https://doi.org/10.1016/j.chemosphere.2019.02.057>.

#### References

- Abdelouas, A., Lutze, W., Nuttal, E., 1998. Chemical reactions of uranium in ground water at a mill tailing site. *J. Contam. Hydrol.* 34, 343–361. [https://doi.org/10.1016/S0169-7722\(98\)00097-7](https://doi.org/10.1016/S0169-7722(98)00097-7).
- Abdelouas, A., Lutze, W., Gong, W., Nuttall, E.H., Strietelmeier, B.A., Travis, B.J., 2000. Biological reduction of uranium in groundwater and subsurface soil. *Sci. Total Environ.* 250, 21–35. [https://doi.org/10.1016/S0048-9697\(99\)00549-5](https://doi.org/10.1016/S0048-9697(99)00549-5).
- Abdelouas, A., 2006. Uranium mill tailings : geochemistry, mineralogy, and environmental impact. *Elements* 2, 335–341. <https://doi.org/10.2113/gselements.2.6.335>.
- Akhtar, N., Tufail, M., Ashraf, M., 2005. Natural environmental radioactivity and estimation of radiation exposure from saline soils. *Int. J. Environ. Sci. Technol.* 1 (4), 279–285. <https://doi.org/10.1007/BF03325843>.
- Balonov, M., 2008. Exposures from environmental radioactivity: international safety standards. *Appl. Radiat. Isot.* 68, 1546–1549. <https://doi.org/10.1016/j.apradiso.2007.10.013>.
- Blanco Rodríguez, P., Lozano, J.C., Vera Tomé, F., Prieto, C., Medeiros, A., 2018. Influence of soil conditions on the distribution coefficients of  $^{226}\text{Ra}$  in natural soils. *Chemosphere* 205, 188–193. <https://doi.org/10.1016/j.chemosphere.2018.04.093>.
- Blasco, M., Gázquez, M.J., Pérez-Moreno, S.M., Grande, J.A., Valente, T., Santisteban, M., de la Torre, M.L., Bolívar, J.P., 2016. Polonium behaviour in reservoirs potentially affected by acid mine drainage (AMD) in the Iberian pyrite belt (SW of Spain). *J. Environ. Radioact.* 152, 60–69. <https://doi.org/10.1016/j.jenvrad.2015.11.008>.
- Bollhöfer, A., Beraldo, A., Pftzner, K., Espano, A., Doering, C., 2014. Determining a pre-mining radiological baseline from historic airborne gamma surveys: a case study. *Sci. Total Environ.* 468–469, 764–773. <https://doi.org/10.1016/j.scitotenv.2013.09.001>.
- Carvalho, F.P., Madruga, M.J., Reis, M.C., Alves, J.G., Oliveira, J.M., Gouveia, J., Silva, L., 2007. Radioactivity in the environment around past radium and uranium mining sites of Portugal. *J. Environ. Radioact.* 96, 39–46. <https://doi.org/10.1016/j.jenvrad.2007.01.016>.
- Carvalho, F., 2014. The national radioactivity monitoring program for the regions of uranium mines and uranium legacy sites in Portugal. *Procedia Earth Planet. Sci.* 8, 33–37. <https://doi.org/10.1016/j.proeps.2014.05.008>.
- Carvalho, F.P., Oliveira, J.M., Malta, M., Lemos, M.E., 2014. Radioanalytical assessment of environmental contamination around non-remediated uranium mining legacy site and radium mobility. *J. Radioanal. Nucl. Chem.* 299, 119–125. <https://dx.doi.org/10.1007/s10967-013-2734-1>.
- Carvalho, J., Diamantino, C., Rosa, C., Carvalho, E., 2016. Potential recovery of mineral resources from mining tailings of abandoned mines in Portugal. In: *3rd International Symposium on Enhanced Landfill Mining*, pp. 501–516.
- EDM, 2011. The legacy of abandoned mines. In: EDM, DCEG (Eds.), *The Context and the Action in Portugal*. ISBN 978-972-95226-2-8.
- Fernandes, A.C., Santos, J.P., Marques, J.G., Kling, A., Ramos, A.R., Barradas, N.P., 2010. Validation of the Monte Carlo model supporting core conversion of the Portuguese Research Reactor (RPI) for neutron fluence rate determinations. *Ann. Nucl. Energy* 37, 1139–1145. <https://doi.org/10.1016/j.anucene.2010.05.004>.
- Govindaraju, K., 1994. Compilation of working values and sample description for 383 geostandards. *Geostand. Newsl.* 18, 1–158. <https://doi.org/10.1046/j.1365-2494.1998.53202081.x-i1>.
- Grønlie, A., Torsvik, T.H., 1989. On the origin and age of hydrothermal thorium-enriched carbonate veins and breccias in the Møre-Trøndelag Fault Zone, Central Norway. *Nor. Geol. Tidsskr.* 69 (1), 1–19.
- IAEA, 2002. Monitoring and Surveillance of Residues from the Mining and Milling of Uranium and Thorium. Safety Reports Series No 27. International Atomic Energy Agency, Vienna, p. 65.
- ICRP, 1991. 1990 Recommendations of the International Commission on Radiological Protection. ICRP Publication 60, Pergamon Press, Oxford and New York, ISBN 0080411444.
- ICRP, 1999. Protection of the Public in Situations of Prolonged Radiation Exposure, vol. 29. ICRP Publication 82, Oxford and New York. No 1–2, Pergamon Press, 0146–6453.
- Karahan, G., Bayulken, A., 2000. Assessment of gamma dose rates around Istanbul (Turkey). *J. Environ. Radioact.* 47 (2), 213–221. [http://doi.org/10.1016/S0265-931X\(99\)00034-X](http://doi.org/10.1016/S0265-931X(99)00034-X).
- Kamunda, C., Mathuthu, M., Madhuku, M., 2016. An assessment of radiological hazards from gold mine tailings in the province of Gauteng in South Africa. *Int. J. Environ. Res. Public Health* 13, 138. <https://doi.org/10.3390/ijerph13010138>.
- Khatun, R., Saadat, A.H.M., Hasnan, M.M., Akter, S., 2013. Assessment of natural radioactivity and radiation hazard in soil samples of Rajbari district of Bangladesh. *Jahangirnagar Univ. Environ. Bull.* 2, 1–8. <https://doi.org/10.3329/jueb.v2i0.16324>.
- Long, G.J., Cranshaw, T.E., Longworth, G., 1983. The ideal Mössbauer effect absorber thicknesses. *Mossb. Effect. Ref. Data J.* 6, 42–49.
- Marques, R., Prudêncio, M.I., Dias, M.I., Rocha, F., 2011. Patterns of rare earth and other trace elements in different size fractions of clays of Campanian-Maastrichtian deposits from the Portuguese western margin (Aveiro and Taveiro Formations). *Chem. Erde-Geochem.* 71, 337–347. <https://doi.org/10.1016/j.chemer.2011.02.002>.
- Marshall, T.A., Morris, K., Law, G.T.W., Livens, F., Mosselmans, J.F.W., Bots, P., Samuel, S., 2017. Incorporation of uranium into Hematite during crystallization



- from ferrihydrite. *Environ. Sci. Technol.* 48, 3724–3731. <https://doi.org/10.1021/es500212a>.
- Mora, P., Picado, E., Minato, S., 2007. Natural radiation doses for cosmic and terrestrial components in Costa Rica. *Appl. Radiat. Isot.* 65 (1), 79–84. <https://doi.org/10.1016/j.apradiso.2006.06.001>.
- Naamoum, T., Degering, D., Hebert, D., 2002. Mobility of radionuclides in the uranium tailings “Schneckenstein” (Germany). In: *Tailings and Mine Waste '02: Proceedings of the 9th International Conference, Fort Collins, Colorado*. Sweets & Zeitlinger, Balkema Publishers., CRC Press, ISBN 9789058093530, p. 532.
- Ohnuki, T., Kozai, N., Samadfam, M., Yasuda, R., Yamamoto, S., Narumi, K., Naramoto, H., Murakami, T., 2004. The formation of autunite (Ca(UO<sub>2</sub>)<sub>2</sub>(PO<sub>4</sub>)<sub>2</sub>·nH<sub>2</sub>O) within the leached layer of dissolving mechanism of uranium by apatite. *Chem. Geol.* 211, 1–14. <https://doi.org/10.1016/j.chemgeo.2004.03.004>.
- Op de Beeck, J., 1972. GELIAN Program. Institute for Nuclear Sciences, University of Ghent, Belgium.
- Op de Beeck, J., 1974. OLIVE Program. Institute for Nuclear Sciences, University of Ghent, Belgium.
- Prudêncio, M.I., Valente, T., Marques, R., Sequeira Braga, M.A., Pamplona, J., 2015. Geochemistry of rare earth elements in a passive treatment system built for acid mine drainage remediation. *Chemosphere* 138, 691–700. <https://doi.org/10.1016/j.chemosphere.2015.07.064>.
- Rochedo, E.R.R., Lauria, D., 2008. International versus national regulations: concerns and trends. *Appl. Radiat. Isot.* 66, 1550–1553. <https://doi.org/10.1016/j.apradiso.2007.10.014>.
- Rodríguez, P.B., Tomé, F.V., Lozano, J.C., 2014. Assessment of the vertical distribution of natural radionuclides in a mineralized uranium area in south-west Spain. *Chemosphere* 95, 527–534. <https://doi.org/10.1016/j.chemosphere.2013.09.111>.
- Silver Turyahabwa, E.R., Jurua, E., Oriada, R., Mugaiga, A., Bem Enjiku, D.D., 2016. Determination of natural radioactivity levels due to mine tailings from selected mines in southwestern Uganda. *J. Environ. Earth Sci.* 6, 154–163. ISSN 2224-3216 (Paper) ISSN 2225-0948 (Online).
- Sima, O., Arnold, D., Dovlete, C., 2001. GESPECOR—a versatile tool in gamma-ray spectrometry. *J. Radioanal. Nucl. Chem.* 248 (2), 359–364. <https://doi.org/10.1023/A:1010619806898>.
- Tuovinen, H., Pohjolainen, E., Vesterbacka, D., Kaksonen, K., Virkanen, J., Solatie, D., Lehto, J., Read, D., 2016. Release of radionuclides from waste rock and tailings at a former pilot uranium mine in eastern Finland. *Boreal Environ. Res.* 21, 471–480. ISSN 1239-6095 (print) ISSN 1797-2469 (online). <https://helda.helsinki.fi/handle/10138/172377>.
- UNSCEAR, 2000. Sources and Effects of Ionizing Radiation. United Nations Scientific Committee on the Effects of Atomic Radiation, Annex B: Exposures from Natural Radiation Sources, vol. I. United Nations Publications, New York, p. 644.
- UNSCEAR, 2008. Sources and Effects of Ionizing Radiation. United Nations Scientific Committee on the Effects of Atomic Radiation, Annex B: Exposures of the Public and Workers from Various Sources of Radiation, vol. I. United Nations Publications, New York, p. 143.
- Usikalu, M.R., Anoka, O.C., Balogun, F.A., 2011. Radioactivity measurements of the Jos tin mine tailing in northern Nigeria. *Arch. Phys. Res.* 2 (2), 80–86, 0976–0970.
- Valente, T. Maria, Leal Gomes, C., 2009a. Occurrence, properties and pollution potential of environmental minerals in acid mine drainage. *Sci. Total Environ.* 407, 1135–1152. <https://doi.org/10.1016/j.scitotenv.2008.09.050>.
- Valente, T. Maria, Leal Gomes, C., 2009b. Fuzzy modelling of acid mine drainage environments using geochemical, ecological and mineralogical indicators. *Environ. Geol.* 57 (3), 653–663. <https://doi.org/10.1007/s00254-008-1344-7>.
- Valente, T., Gomes, P., Sequeira Braga, M.A., Dionísio, A., Pamplona, J., Grande, J.A., 2015. Iron and arsenic-rich nanoprecipitates associated with clay minerals in sulfide-rich waste dumps. *Catena* 131, 1–13. <https://doi.org/10.1016/j.catena.2015.03.009>.
- Vandenhove, H., 2000. European sites contaminated by residues from the ore extracting and processing industries. In: *Restoration of Environments with Radioactive Residues*. Proceedings Series. STI/PUB/1092. IAEA, Vienna, pp. 61–89.
- Waerenborgh, J.C., Rojas, D.P., Shaula, A.L., Mather, G.C., Patrakeev, M.V., Kharton, V.V., Frade, J.R., 2005. Phase formation and iron oxidation state in SrFe(Al)O<sub>3-δ</sub> perovskites. *Mater. Lett.* 59, 1644–1648. <https://doi.org/10.1016/j.matlet.2005.01.033>.
- Wentworth, C.K., 1922. A scale of grade and class terms for clastic sediments. *J. Geol.* 30 (5), 377–392.

## Web references

- EDM – Empresa de Desenvolvimento Mineiro, SA <http://edm.pt/>.